
Spread them Apart: Towards Robust Watermarking of Generated Content

Mikhail Pautov^{1,2*}

Danil Ivanov^{3*}

Andrey V. Galichin^{1,3}

Oleg Rogov^{1,3,4}

Ivan Oseledets^{1,3}

¹AIRI, Moscow, Russia

²ISP RAS Research Center for Trusted AI, Moscow, Russia

³Skolkovo Institute of Science and Technology, Moscow, Russia

⁴Moscow Technical University of Communications and Informatics, Moscow, Russia

Abstract

Generative models that can produce realistic images have improved significantly in recent years. The quality of the generated content has increased drastically, so sometimes it is very difficult to distinguish between the real images and the generated ones. Such an improvement comes at a price of ethical concerns about the usage of the generative models: the users of generative models can improperly claim ownership of the generated content protected by a license. In this paper, we propose an approach to embed watermarks into the generated content to allow future detection of the generated content and identification of the user who generated it. The watermark is embedded during the inference of the model, so the proposed approach does not require the retraining of the latter. We prove that watermarks embedded are guaranteed to be robust against additive perturbations of a bounded magnitude. We apply our method to watermark diffusion models and show that it matches state-of-the-art watermarking schemes in terms of robustness to different types of synthetic watermark removal attacks.

1 INTRODUCTION

Recent advances in generative models have brought the performance of image synthesis tasks to a whole new level. For example, the quality of the images generated by diffusion models (DMs, Croitoru et al. [2023], Rombach et al. [2022], Esser et al. [2024]) is now sometimes comparable to the one of the human-generated pictures or photographs. Compared to generative adversarial networks (GANs, Goodfellow et al. [2014], Brock et al. [2019]), diffusion models allow the generation of high-resolution, naturally looking

pictures and incorporate much more stable training, leading to a more diverse generation. More than that, the image generation process with diffusion models is more stable, controllable, and explainable. They are easy to use and are widely deployed as tools for data generation, image editing (Kawar et al. [2023], Yang et al. [2023]), music generation (Schneider et al. [2024]), text-to-image synthesis (Saharia et al. [2022], Zhang et al. [2023], Ruiz et al. [2023]) and in other multimodal settings.

Unfortunately, several ethical and legal issues may arise from the usage of diffusion models. On the one hand, since diffusion models can be used to generate fake content, for example, deepfakes (Zhao et al. [2021], Narayan et al. [2023]), it is crucial to develop automatic tools to verify that a particular digital asset is artificially generated. On the other hand, a dishonest user of the model protected by a copyright license can query it, receive the result of generation, and later claim exclusive copyright. In this work, we focus on the detection of the content generated by a particular model and the identification of the end-user who queried the model to generate a particular content. We develop a technique to embed the digital watermark into the generated content during the inference of the generative model, so it does not require retraining or fine-tuning the generative model. The approach allows not only to verify that the content was generated by a source model but also to identify the user who sent a corresponding query to the generative model. We prove that the watermark embedded is robust against additive perturbations of the content of a bounded magnitude.

Our contributions are threefold:

- We propose *Spread them Apart*, the framework to embed digital watermarks into the generative content of continuous nature. Our method embeds the watermark during the process of content generation and, hence, does not require additional training of the generative model.
- We apply the framework to watermark images gener-

*Equal contribution.

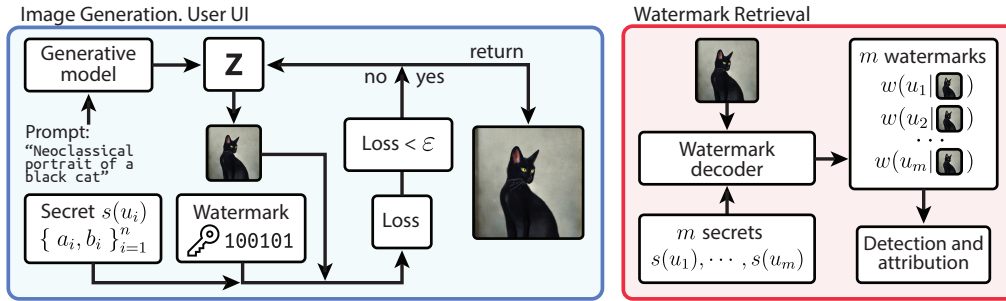


Figure 1: Illustration of the proposed method. During the image generation phase, the user u_i queries the model with the prompt. Given the prompt, the model produces the latent z , from which the image is generated. If the image generated satisfies the constraint $\mathcal{L}_{wm} < \epsilon$ (meaning the watermark is successfully embedded), it is yielded to the user; otherwise, the loss function from Eq. 10 is minimized with respect to the latent z . Note that the value of ϵ may vary from image to image. During the watermark retrieval phase, given the image x and m secrets, $s(u_1), \dots, s(u_m)$, the watermark decoder extracts m watermarks, $w(u_1|x), \dots, w(u_m|x)$. Then, the image is attributed to the user u according to the Eq. 9.

ated by a diffusion model and prove that the watermark embedded is provably robust to the additive perturbations of a bounded magnitude that can be applied during the post-processing of the image.

- Experimentally, we show that our approach outperforms competitors in terms of the robustness to different types of post-processing of the images aimed at watermark removal, such as brightness and contrast adjustment or gamma correction.

2 RELATED WORK

2.1 DIFFUSION MODEL

Inspired by non-equilibrium statistical physics, Sohl-Dickstein et al. [2015] introduced the diffusion model to fit complex probability distributions. Ho et al. [2020] introduced a new class of models called Denoising Diffusion Probabilistic Models (DDPM) by establishing a novel connection between the diffusion model and the denoising scoring matching. Later, the Latent Diffusion Model (LDM) was developed to improve efficiency and reduce computational complexity, with the diffusion process happening within a latent space Rombach et al. [2022]. During training, the LDM uses an encoder \mathcal{E} to map an input image x to the latent space: $z = \mathcal{E}(x)$. For the reverse operation a decoder \mathcal{D} is employed, so that $x = \mathcal{D}(z)$. During inference, the LDM starts with a noise vector $z \sim \mathcal{N}(0, I)$ in the latent space and iteratively denoises it. The decoder then maps the final latent representation back to the image space.

2.2 WATERMARKING OF DIGITAL CONTENT

Watermarking has been recently adopted to protect the intellectual property of neural networks (Wu et al. [2020], Pautov et al. [2024]) and generated content (Kirchenbauer

et al. [2023], Zhao et al. [2024], Fu et al. [2024]). In a nutshell, watermarking of generated content is done by injection of digital information within the generated image allowing the subsequent extraction. Existing methods of digital content watermarking can be divided into two categories: content-level watermarking and model-level watermarking. The methods of content-level watermarking operate in some representation of content, for example, in the frequency domain of the image signal (Ó Ruanaidh et al. [1996], Cox et al. [1996]). When the image is manipulated in the frequency domain, the watermark embedding process can be adapted to produce watermarks that are robust to geometrical image transformations, such as rotations and translations (Wen et al. [2024]). Model-level watermarking approaches are designed to embed information during the generation process. In end-to-end methods, the models to embed and extract watermark are learned jointly (Zhu et al. [2018], Hayes and Danezis [2017]). In Yu et al. [2021], it was proposed to teach the watermark encoder on the training data of the generative model; such an approach yields a watermarking scheme that is conditioned on the generative model and its training dataset. This method was later adapted to latent diffusion models (Fernandez et al. [2023]) and unconditional diffusion models (Zhao et al. [2023]). In contrast, there are methods that do not require additional model training. These methods are designed to alter the output distribution of the generative model to embed previously learned watermark into the model or the content itself (Kirchenbauer et al. [2023], Wen et al. [2024]).

2.3 ROBUSTNESS TO WATERMARK REMOVAL ATTACKS

Watermarking attacks are aimed at removing the watermark embedded into the model’s weights or generated content. In the prior works on removing the watermarks from generated images (Li et al. [2019], Cao et al. [2019]), the at-

tack problem is formulated in terms of the image-to-image translation task, and methods to remove watermarks via an auxiliary generative adversarial network are presented. Other approaches (Hertz et al. [2019], Liang et al. [2021], Sun et al. [2023]) perform watermark removal in two steps: firstly, the visual watermark is localized within an image; secondly, it is removed via a multi-task learning framework.

In practice, watermarking scheme has to be robust to destructive and constructive attacks, or synthetic transformations of the data. Destructive transformations, such as brightness and contrast adjustment, geometric transformations, such as rotations and translations, compression methods, and additive noise are aimed at watermark removal by applying a transformation. In contrast, constructive attacks treat watermarks as noise and are aimed at the restoration of original content (Zhang et al. [2024]). It is usually done by applying purification techniques, such as Gaussian blur (Hosam [2019]) or image inpainting (Liu et al. [2021], Xu et al. [2017]).

Signal Processing Attacks focus on noise addition, compression, and filtering. Robust watermarking schemes based on frequency domain transformations and randomizing offered higher resilience against these types of attacks (Taran et al. [2019]).

3 PROBLEM STATEMENT

In this section, we formulate the problem statement and the research objectives. Note that we focus on the watermarking of images generated by diffusion models, but the formulation below is valid for watermarking of any generated content, for example, audio, video, or text.

3.1 IMAGE WATERMARKING

In our approach, we focus on *detection* and *attribution* of the generated image simultaneously: while detection is aimed to verify whether a particular image is generated by a given model, attribution is aimed at determining the user who generated the image.

Suppose that we are given the generative model f deployed in the black-box setting, i.e., as a service: in the generation phase a user $u_i \in [u_1, \dots, u_m]$ sends a query to the model and receives a generated image $x \in \mathbb{R}^d$. If x is a watermarked image, the owner of model f should be able to identify that x is generated by user u_i by querying the model f . In our method, the image is watermarked during the *generation* phase, not during the post-processing. We formulate the process of watermarking and attribution in the following way:

1. When the user $u_i \in [u_1, \dots, u_m]$ registers in the service, it is assigned a pair of *public* and *private* keys, namely, the watermark $w(u_i)$ and the secret $s(u_i)$. Wa-

termark is a binary string of length n and the secret is the sequence of tuples of length n , where each tuple is a pair of unique positive numbers treated as indices: $w(u_i) \in \{0, 1\}^n$, $s(u_i) \in \mathbb{Z}_+^{2n}$.

2. When the user u_i queries the model f , it generates the image x with the watermark $w(u_i)$ embedded into x .
3. When the watermarked object x is received by the model owner, it extracts the watermark $w(u_i|x)$ using the secret $s(u_i)$ of the user u_i and compares it with the watermark $w(u_i)$ assigned to the user u_i . Following the previous works (Yu et al. [2021], Fernandez et al. [2023]), we compute the bitwise distance $d(w(u_i|x), w(u_i))$ between $w(u_i|x)$ and $w(u_i)$:

$$d(w(u_i|x), w(u_i)) = \sum_{j=1}^n \mathbb{1}(w(u_i|x)_j \neq w(u_i)_j). \quad (1)$$

Remark. For robustness to watermark removal attack, in case of a single user u_i , we flag the object x as generated by the user u_i if the distance $d(w(u_i|x), w(u_i))$ is either small or large, namely, if

$$d(w(u_i|x), w(u_i)) \in [0, \tau_1] \cup [\tau_2, n], \quad (2)$$

where $\tau_1 \ll n$ and $\tau_2 \gg 0$. This procedure is known as the double-tail detection (Jiang et al. [2023]).

3.2 THE PROBABILITY OF INCORRECT ATTRIBUTION

We assume that the watermark $w(u_i)$ attributed to the user u_i is drawn randomly and uniformly from the set of all possible n -bit watermarks, $\{0, 1\}^n$. Following the prior works (Fernandez et al. [2023]), we formulate the detection problem as the hypothesis test. In case of a single user u_i , we define the null hypothesis \mathcal{H}_0 = ‘‘the object x is generated not by u_i ’’ and the alternative hypothesis \mathcal{H}_1 = ‘‘the object x is generated by u_i ’’. Additionally, under the null hypothesis, we assume that the j 'th bit in the watermark $w(u_i|x)$ extracted from x is the same as the j 'th bit from $w(u_i)$ with the probability p_i .

In the case of a single user u_i and given the attribution rule from the Eq. 2, we compute the probability of the false attribution, namely,

$$FRP(1)|_{u_i} = \mathbb{P}[d(w', w(u_i)) \in [0, \tau_1] \cup [\tau_2, n]] = \sum_{q \in [0, \tau_1] \cup [\tau_2, n]} \binom{n}{q} p_i^q (1 - p_i)^{n-q}, \quad (3)$$

where $w' = w(u_i|x)$ is a random watermark uniformly sampled from $\{0, 1\}^n$, namely, $w' \sim \{0, 1\}^n$, $w' \neq w(u_i)$.

In case of m users, the probability $FPR(m)$ of incorrect attribution of the non-watermarked image x to some other

user $u_j \in [u_1, \dots, u_m]$ is upper bounded by the probability below:

$$\begin{aligned} FPR(m) &\leq \mathbb{P}_{w' \sim \{0,1\}^n} [\exists u_j \in [u_1, \dots, u_m] : \\ d(w', w(u_j)) &\in [0, \tau_1] \cup [\tau_2, n]] \leq \\ &\sum_{u_j \in [u_1, \dots, u_m]} FPR(1)|_{u_j} = \hat{p}. \end{aligned} \quad (4)$$

Note that this upper bound holds regardless of the independence of random variables ξ_1, \dots, ξ_m , where

$$\xi_i = \mathbb{1}[d(w(u_i|x), w(u_i)) \in [0, \tau_1] \cup [\tau_2, n]]. \quad (5)$$

Remark. In our experiments, the probability p_i from above is estimated to be close to $\frac{1}{2}$.

3.3 ROBUSTNESS TO WATERMARK REMOVAL ATTACKS

When the user u_i receives the watermarked image x , it can post-process it to obtain the other image, x' , which does retain the sufficient part of the watermark $w(u_i)$. The transition from x to x' may be done by applying an image transformation, such as brightness or contrast adjustment, Gaussian blur, or additive noise. The other approach is to perform an adversarial attack on the generative model to erase the watermark (Jiang et al. [2024]). In our settings, we assume that the generative model is deployed as the black-box service with limited access to the API, so an adversary can not apply white-box adversarial attacks (Jiang et al. [2023]).

4 METHOD

In this section, we provide a detailed description of the proposed approach, its implementation details, and the robustness guarantee against additive watermarking removal attacks of bounded magnitude.

4.1 EMBEDDING AND EXTRACTION OF THE WATERMARK

Suppose that f is the generative model. Recall that the user $u_i \in [u_1, \dots, u_m]$ receives a pair $(w(u_i), s(u_i))$ after the registration in the service, where both the watermark and the secret are unknown to the user and are privately kept by the owner of f . Let x be the generated image. Then, the watermark embedding process is described as follows:

1. The secret $s(u_i)$ is interpreted as two sequences of indices, $A = \{a_1, \dots, a_n\}$ and $B = \{b_1, \dots, b_n\}$. The watermark $w(u_i) = \{w_1, \dots, w_n\}$ is the binary string that restricts the generated image x in the areas represented by the sets A and B .

2. The restriction of x in the areas represented by the sets A and B given $w(u_i)$ is the following implication:

$$\begin{cases} w_i = 0 \implies x_{a_i} \geq x_{b_i} \\ w_i = 1 \implies x_{a_i} < x_{b_i}, \end{cases} \quad (6)$$

where x_j is the intensity of the j 'th pixel of x . To increase the robustness to watermark removal attacks, we apply additional regularization to x :

$$\min_{j \in [1, \dots, n]} |x_{a_j} - x_{b_j}| \geq \epsilon, \quad (7)$$

where $\epsilon > 0$ is the scalar parameter.

To perform detection and attribution of the given image x , the owner of the generative model firstly constructs m watermarks $w(u_1|x), \dots, w(u_m|x)$ by reversing the implication from the Eq. 6. Namely, given the secret $s(u_i) = \{a_1, \dots, a_n, b_1, \dots, b_n\}$ of user u_i , the watermark bits are restored by the following rule:

$$\begin{cases} x_{a_j} \geq x_{b_j} \implies w(u_i|x)_j = 0, \\ x_{a_j} < x_{b_j} \implies w(u_i|x)_j = 1. \end{cases} \quad (8)$$

Remark. Here, we distinguish the watermark $w(u_i)$ assigned by the owner of generative model to the user u_i from the watermark $w(u_i|x)$ extracted from the image x with the use of the secret $s(u_i)$ of user u_i .

When m watermarks $w(u_1|x), \dots, w(u_m|x)$ are extracted, the owner of the model assigns x to the user u with the minimum distance $d(w(u_i), w(u_i|x))$ between assigned and extracted watermarks:

$$u = \arg \min_{u_i \in [u_1, \dots, u_m]: \xi_i=1} d(w(u_i), w(u_i|x)), \quad (9)$$

where ξ_i is the indicator function from the Eq. 5. Note that if $\xi_i = 0$ for all $i \in [1, \dots, m]$, then x is identified as image not generated by f .

4.2 IMPLEMENTATION DETAILS

In this subsection, we describe the watermarking procedure. First of all, we have to note that in the Stable Diffusion model, the latent vector z produced by the U-Net is then decoded back into the image space using a VAE decoder: $x = \mathcal{D}(z)$. To embed the watermark into an image, we optimize a special two-component loss function with respect to the latent vector z . The overall loss is written as follows:

$$\mathcal{L} = \lambda_{wm} \mathcal{L}_{wm} + \lambda_{qual} \mathcal{L}_{qual}, \quad (10)$$

The first term, \mathcal{L}_{wm} , defines how the image complies with the pixel difference imposed by the watermark $w(u_i) = \{w_1, \dots, w_n\}$ and the secret $s(u_i) = \{a_1, \dots, a_n, b_1, \dots, b_n\}$:

$$\mathcal{L}_{wm} = \sum_{i=1}^n \min((-1)^{w_i}(x_{a_i} - x_{b_i}) + \varepsilon, 0), \quad x = \mathcal{D}(z), \quad (11)$$

Here, ε defines the minimum difference between private key pixels that we would like to obtain. Note that the larger the value of ε is, the more robust the watermark is to additive perturbations. At the same time, the increase of ε negatively influences the perceptual quality of images.

The second term \mathcal{L}_{qual} , is introduced to preserve the generation quality of the image. The value \mathcal{L}_{qual} is a difference in image quality measured by LPIPS metric (Zhang et al. [2018]), which acts as a regularization. Given x as the original image and \hat{x} as the watermarked image, \mathcal{L}_{qual} is defined as follows:

$$\mathcal{L}_{qual}(x, \hat{x}) = \sum_j \frac{1}{W_j H_j} \sum_{w,h} \|\phi^j(x) - \phi^j(\hat{x})\|_2^2. \quad (12)$$

Here, $\phi^j(x) = w_j \odot o_{hw}^j(x)$, where $o^j(x)$ are the internal activations of the CNN, AlexNet (Krizhevsky et al. [2012]), in our case.

Note that we do not perform denoising at each iteration, as we only manipulate the latent vectors produced by U-Net; the forward step of the described optimization procedure involves only the decoding of the latent vectors: $x = \mathcal{D}(z)$.

The optimization is performed over 700 steps of the Adam optimizer with the learning rate of 8×10^{-3} , where every 100 iteration, the learning rate is halved. When the convergence is reached, the ordinary Stable Diffusion post-processing of the image is performed. The coefficients λ_{wm} and λ_{qual} are determined experimentally and set to be 0.9 and 150, respectively, the value of ε was set to be $\varepsilon = 0.2$. Schematically, the process of watermark embedding and extraction is presented in Figure 1.

4.3 ROBUSTNESS GUARANTEE

By construction, the watermark embedded by our method is robust against additive watermark removal attacks of a bounded magnitude. Namely, let the watermark $w(u_i|x)$ be embedded in x with the use of the secret $s(u_i) = \{a_1, \dots, a_n, b_1, \dots, b_n\}$ of the user u_i . Let

$$\Delta_i = \frac{|x_{a_i} - x_{b_i}|}{2}. \quad (13)$$

Then, the following lemma holds.

Lemma 4.1. *Let $\varepsilon \in \mathbb{R}^d$ and $\Delta_{i_1} \leq \Delta_{i_2} \leq \dots \leq \Delta_{i_n}$.*

Then, if $\|\varepsilon\|_\infty < \Delta_{i_k}$, then $d(w(u_i|x + \varepsilon), w(u_i|x)) < k$.

Proof. Note that to change the j 'th bit of watermark $w(u_i|x)$, an adversary has to change the sign in expression $(x_{a_j} - x_{b_j})$. Without the loss of generality, let $x_{a_j} - x_{b_j} \geq 0$.

Consider an additive noise ε such that $(x + \varepsilon)_{a_j} - (x + \varepsilon)_{b_j} < 0$, meaning $|\varepsilon_{b_j} - \varepsilon_{a_j}| > |x_{a_j} - x_{b_j}|$. Note that $\|\varepsilon\|_\infty \geq \max(|\varepsilon_{a_j}|, |\varepsilon_{b_j}|)$.

If $\max(|\varepsilon_{a_j}|, |\varepsilon_{b_j}|) < \Delta_j$, then $|\varepsilon_{b_j} - \varepsilon_{a_j}| \leq |\varepsilon_{b_j}| + |\varepsilon_{a_j}| < 2\Delta_j = |x_{a_j} - x_{b_j}|$, yielding a contradiction. Thus, $\|\varepsilon\|_\infty \geq \Delta_j$.

Finally, an observation that all the indices in $s(u_i)$ are unique finalizes the proof. \square

This lemma provides a lower bound on the l_∞ norm of the additive perturbation ε applied to x which is able to erase at least k bits of the watermark $w(u_i|x)$ embedded into x .

5 EXPERIMENTS

5.1 GENERAL SETUP

We use `stable-diffusion-2-base` model (Romach et al. [2022]) with the `epsilon` prediction type and 50 steps of denoising for the experiments. The resolution of generated images is 512×512 . The experiments were conducted on `DiffusionDB` dataset (Wang et al. [2022]). Specifically, we choose 1000 unique prompts and generate 1000 different images.

The public key for the user is sampled from the Bernoulli distribution with the parameter $p = 0.5$. The length of a key is set to be $n = 100$. The private key is generated by randomly picking $2n$ unique pairs of indices of the flattened image.

5.2 ATTACK DETAILS

We evaluate the robustness of the watermarks embedded by our method against the following watermark removal attacks: brightness adjustment, contrast shift, gamma correction, image sharpening, hue adjustment, saturation adjustment, random additive noise, JPEG compression, and the white-box PGD adversarial attack (Madry et al. [2018]). In this section, we describe these attacks in detail.

Brightness adjustment of an image x was performed by adding a constant value to each pixel: $x_{brightness} = x + b$, where b was sampled from the uniform distribution $\mathcal{U}[-20, 20]$.

Contrast shift was done in two ways: positive and negative. The positive contrast shift implies the multiplication of each pixel of an image by a constant positive factor: $x_{contrast} = cx$, where c was sampled from the uniform distribution, $c \sim \mathcal{U}[0.5, 2]$.

On the contrary, when the contrast shift is performed with the negative value of c (namely, $c \sim \mathcal{U}[-2, -0.5]$), such a transform turns an image into a negative. Later, we treat

these transforms separately and denote them as “Contrast +” and “Contrast −”, depending on the sign of c .

Gamma correction is nothing but taking the exponent of each pixel of the image: $x_{gamma} = x^g$, where $g \sim \mathcal{U}[0.5, 2]$.

For sharpening, hue, and saturation adjustment, we use implementations from the `KORNIA` package (Riba et al. [2020]) with the following parameters: $a_{saturation} = 2$, $a_{hue} = 0.2$, $a_{sharpness} = 2$.

The noise for the noising attack was sampled from the uniform distribution $\mathcal{U}[-\delta, \delta]$, where $\delta = 25$. Note, that the maximum $\|\cdot\|_\infty$ of noise is then equal to 25.

JPEG compression was performed using DiffJPEG (Shin [2017]) with quality equal to 50.

White-box attack aims to change the embedded watermark w to some other watermark \tilde{w} by optimizing the image with respect to the loss initially used to embed the watermark w :

$$\begin{aligned} \mathcal{L}_{wb} &= \lambda_{wm} \mathcal{L}_{wm} + \lambda_{qual} \mathcal{L}_{qual}, \quad \text{where} \quad (14) \\ \mathcal{L}_{wm} &= \sum_{i=1}^n \min((-1)^{\tilde{w}_i} (x_{a_i} - x_{b_i}) + \varepsilon, 0). \end{aligned}$$

In Eq. 14, the term \mathcal{L}_{qual} corresponds to the difference in image quality in terms of LPIPS metric, namely,

$$\mathcal{L}_{qual} = LPIPS(x, \hat{x}), \quad (15)$$

where x and \hat{x} are the original image and image on a particular optimization iteration, respectively.

The loss function \mathcal{L}_{wb} pushes the private key pixels to be aligned with a new randomly sampled public key \tilde{w} so that the ground-truth watermark w gets erased. The attack’s budget is the upper bound of $\|\cdot\|_\infty$ norm of the additive perturbation, that we have taken to be $\varepsilon/2$ from the Eq. 11. Let \tilde{x} be the image obtained after the attack. If at some iteration the distance between the source image x and the attacked one \tilde{x} exceeds $\varepsilon/2$, \tilde{x} is being projected back onto the sphere $\|\tilde{x} - x\|_\infty = \varepsilon/2$. The optimization took place for 10 iterations with the Adam optimizer and the learning rate was equal to 10^{-1} . Note that this attack setting implies knowledge about the private key and assumes white-box access to the generative model. Hence, this is de facto the strongest watermark removal attack we consider.

Pixels of the images perturbed by the attacks are then linearly mapped to $[0, 255]$ segment:

$$x^{(i)} = 255 \frac{x^{(i)} - x_{min}^{(i)}}{x_{max}^{(i)} - x_{min}^{(i)}}, \quad i \in \{R, G, B\}. \quad (16)$$

5.3 RESULTS

In this section, we provide the quantitative results of experiments. We report (i) quality metrics of the generated images

(SSIM, PSNR, FID and LPIPS) to evaluate the invisibility of the watermarks, (ii) bit-wise error of the watermark extraction caused by watermark removal attacks and (iii) True Positive Rates in attribution and detection problems.

We compare our results (where applicable) to that of Stable Signature Fernandez et al. [2023], SSL watermarking Fernandez et al. [2022], AquaLora Feng et al. [2024] and WOUAF Kim et al. [2024], one of the state-of-the-art watermarking approaches. In these works the watermark length is set to be 48, 30, 48, and 32, respectively, while we have 100 bits long watermarks: note that the longer the watermark, the harder it is to be embedded.

The image quality metrics are presented in Table 4. It can be seen that our results are comparable to the ones of the baseline methods in terms of the quality of the produced images. A qualitative comparison of original and watermarked images can be found in Figure 2. To evaluate the robustness of the watermarks against removal attacks, we report an average bit-wise error, ABWE:

$$ABWE = \frac{1}{Nn} \sum_{i=1}^N \sum_{j=1}^n \mathbb{1}[w_{i,j}^{gt} \neq w_{i,j}^{extracted}], \quad (17)$$

where $w_{i,j}^{gt}$ and $w_{i,j}^{extracted}$ are the j -th bits of ground truth and extracted private keys, corresponding to the i -th image. Here, n is the number of bits in the watermark and N is the number of images. We report ABWE in Table 1.

To estimate the TPR in the attribution problem, we extract $k = 10$ different watermarks from the watermarked images. To extract a different watermark, we randomly generate $k = 10$ different private keys to simulate other users. The results are reported in Table 2 together with the TPRs under different watermark removal attacks. Note that the PGD attack in this setting is aimed at restoring the original watermark. To estimate the TRP in the watermark detection problem, we do the same procedure for non-watermarked images generated by the Stable Diffusion model and extract $k = 10$ different watermarks. The results are presented in Table 3.

Note that our framework yields both low misattribution and misdetection rates according to the two-tail detection and attribution rules from the Eq. 9. The proposed approach yields watermarks that are provably robust to additive perturbations of a bounded magnitude, multiplicative perturbations of any kind, and exponentiation.

5.4 INCREASING THE ROBUSTNESS TO WATERMARK REMOVAL ATTACKS

It is noteworthy that the set of watermark removal attacks described in Section 5.2 does not include geometric transformations. The version of the proposed method described in Section 4 does not provide robustness against geometric

Table 1: Average bit-wise error after watermark removal attacks. The column ‘‘Generation’’ corresponds to the average bit-wise error of the watermarking process. The best results are highlighted in **bold**.

Method	Generation	Brightness	Contrast +	Contrast -	Gamma	JPEG
Ours	0.0008	0.002	0.002	0.998	0.003	0.147
Stable signature	0.01	0.03	0.02	—	—	0.12
SSL watermarking	0.00	0.06	0.04	—	—	0.04
AquaLora	0.0721	0.137	0.137	—	—	0.0508
Method	Hue	Saturation	Sharpness	Noise	PGD	
Ours	0.01	0.1	0.0008	0.057	0.064	
Stable signature	—	0.01	0.01	—	—	
SSL watermarking	0.06	—	—	—	—	
AquaLora	0.137	0.137	—	0.07	—	

Table 2: TPRs under different types of watermark removal attacks, attribution problem. We use $k = 10$ different private keys and fix $FPR = 10^{-6}$. Such a FPR is achieved when $\tau_1 = 25$ and $\tau_2 = 75$ from Eq. 5. The parameters of removal attacks are presented in Section 5.2. The best results are highlighted in **bold**.

Method	Generation	Brightness	Contrast +	Contrast -	Gamma	JPEG
Ours	1.000	1.000	1.000	1.000	1.000	0.444
Stable signature	0.998	0.927	0.984	—	—	0.784
AquaLora	0.998	0.941	0.941	—	—	0.998
WOUAF	1.000	0.975	—	—	—	0.969
Method	Hue	Saturation	Sharpness	Noise	PGD	
Ours	1.000	0.653	1.000	0.971	0.862	
Stable signature	—	0.998	—	0.776	0.747	
AquaLora	0.941	0.941	—	0.958	—	
WOUAF	—	—	—	0.970	—	

Table 3: TPRs under different types of watermark removal attacks, detection problem. We use $k = 10$ different private keys and fix $FPR = 10^{-6}$. Such a FPR is achieved when $\tau_1 = 25$ and $\tau_2 = 75$ from Eq. 5. The parameters of removal attacks are presented in Section 5.2. The best results are highlighted in **bold**.

Method	Generation	Brightness	Contrast +	Contrast -	Gamma	JPEG
Ours	1.000	1.000	1.000	1.000	1.000	0.444
Stable signature	1.000	0.862	0.984	—	—	0.217
SSL watermarking	1.000	0.940	0.960	—	—	0.810
Method	Hue	Saturation	Sharpness	Noise	PGD	
Ours	1.000	0.653	1.000	0.971	0.862	
Stable signature	—	0.998	—	0.406	0.505	
SSL watermarking	1.000	—	—	—	—	

transformations of the image, however, the method can be extended to support them. In Section A of the supplementary, we discuss an extension of the proposed method to provide robustness against rotations, and translations. An extension is based on a simultaneous embedding of the watermark in the pixel space and special functions, which are invariant to

certain transformations. An intuition behind this extension is as follows. Suppose that the transform $\gamma : \mathbb{R}^d \rightarrow \mathbb{R}^d$ is invariant under parametric perturbation $\phi : \mathbb{R}^d \times \Theta \rightarrow \mathbb{R}^d$, namely, $\gamma(x) = \gamma(\phi(x, \theta))$ for all $x \in \mathbb{R}^d$, $\theta \in \Theta$. Then, if the watermark is successfully embedded into $\gamma(x)$ it becomes robust under perturbation ϕ .

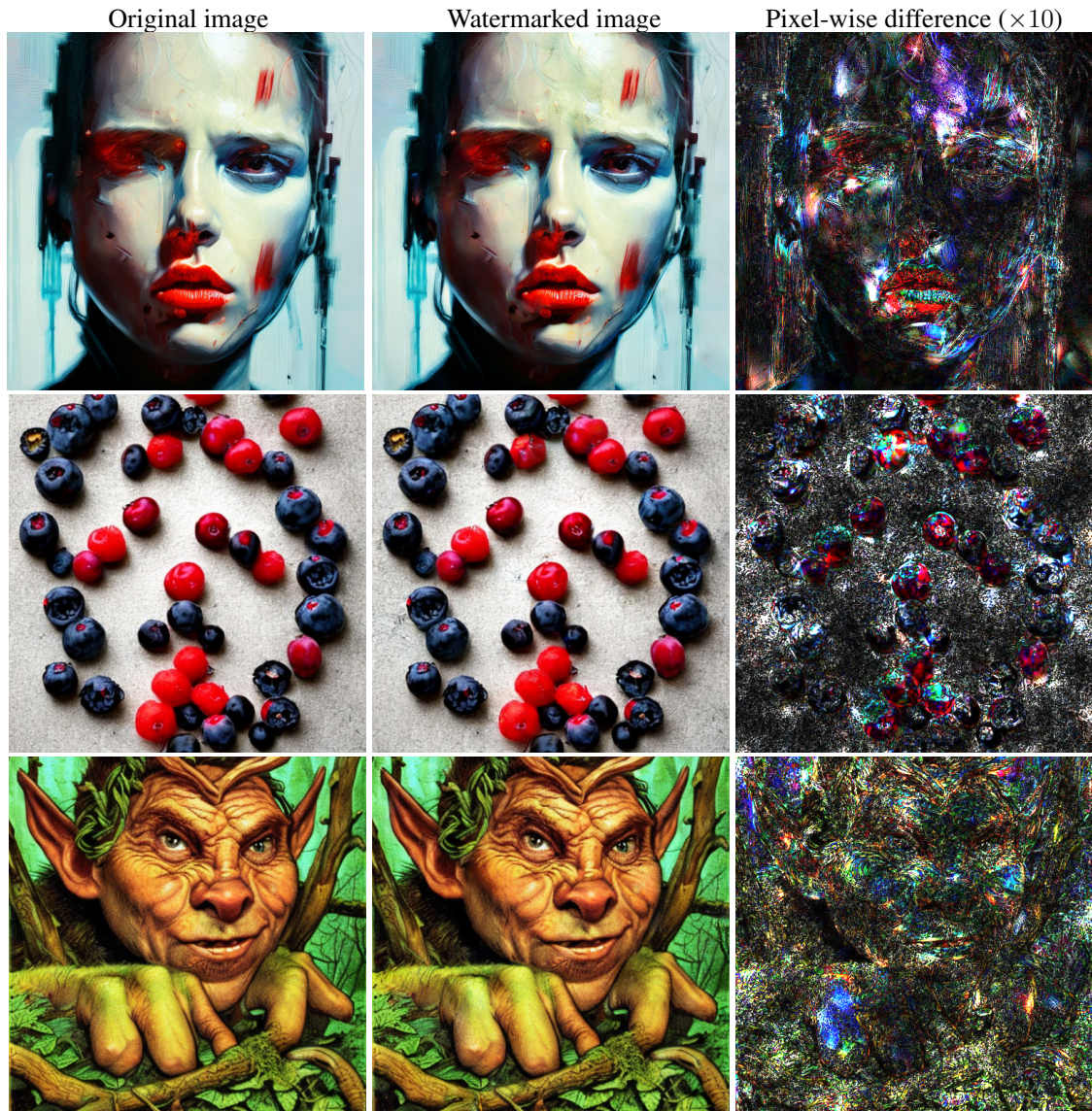


Figure 2: Examples of watermarked images. The maps of absolute pixel-wise difference between source images and the generated ones were added for illustrational purposes.

Table 4: Image quality metrics. The best results are highlighted in **bold**.

Metric	St. Sign.	AquaLora	WOUAF	Ours
SSIM \uparrow	0.89	0.92	—	0.86
PSNR \uparrow	30.0	29.42	—	29.4
FID \downarrow	19.6	24.72	> 15.0	13.2
LPIPS \downarrow	—	—	—	0.0072

6 CONCLUSION AND FUTURE WORK

In this paper, we propose *Spread them Apart*, the framework to watermark generated content of continuous nature and apply it to images generated by Stable Diffusion. We prove that the watermarks produced by our method are provably robust against additive watermark removal attacks of a bounded norm and are provably robust to multiplicative perturbations by design. Our approach can be used to both detect that the image is generated by a given model and to identify the end-user who generated it. Experimentally, we show that our method is comparable to the state-of-the-art watermarking methods in terms of the invisibility of watermark and the robustness to synthetic watermark removal attacks.

References

- Andrew Brock, Jeff Donahue, and Karen Simonyan. Large scale GAN training for high fidelity natural image synthesis. In *7th International Conference on Learning Representations*, 2019.
- Zhiyi Cao, Shaozhang Niu, Jiwei Zhang, and Xinyi Wang. Generative adversarial networks model for visible watermark removal. *IET Image Processing*, 13(10):1783–1789, 2019.
- Ingemar J Cox, Joe Kilian, Tom Leighton, and Talal Shamoon. Secure spread spectrum watermarking for images, audio and video. In *Proceedings of 3rd IEEE International Conference on Image Processing*, volume 3, pages 243–246. IEEE, 1996.
- Florinel-Alin Croitoru, Vlad Hondru, Radu Tudor Ionescu, and Mubarak Shah. Diffusion models in vision: A survey. *IEEE Transactions on Pattern Analysis and Machine Intelligence*, 45(9):10850–10869, 2023.
- Patrick Esser, Sumith Kulal, Andreas Blattmann, Rahim Entezari, Jonas Müller, Harry Saini, Yam Levi, Dominik Lorenz, Axel Sauer, Frederic Boesel, et al. Scaling rectified flow transformers for high-resolution image synthesis. In *Forty-first International Conference on Machine Learning*, 2024.
- Weitao Feng, Wenbo Zhou, Jiyan He, Jie Zhang, Tianyi Wei, Guanlin Li, Tianwei Zhang, Weiming Zhang, and Nenghai Yu. Aqualora: Toward white-box protection for customized stable diffusion models via watermark lora. *arXiv preprint arXiv:2405.11135*, 2024.
- Pierre Fernandez, Alexandre Sablayrolles, Teddy Furon, Hervé Jégou, and Matthijs Douze. Watermarking images in self-supervised latent spaces. In *ICASSP 2022-2022 IEEE International Conference on Acoustics, Speech and Signal Processing (ICASSP)*, pages 3054–3058. IEEE, 2022.
- Pierre Fernandez, Guillaume Couairon, Hervé Jégou, Matthijs Douze, and Teddy Furon. The stable signature: Rooting watermarks in latent diffusion models. In *Proceedings of the IEEE/CVF International Conference on Computer Vision*, pages 22466–22477, 2023.
- Yu Fu, Deyi Xiong, and Yue Dong. Watermarking conditional text generation for ai detection: Unveiling challenges and a semantic-aware watermark remedy. In *Proceedings of the AAAI Conference on Artificial Intelligence*, volume 38, pages 18003–18011, 2024.
- Ian Goodfellow, Jean Pouget-Abadie, Mehdi Mirza, Bing Xu, David Warde-Farley, Sherjil Ozair, Aaron Courville, and Yoshua Bengio. Generative adversarial nets. *Advances in Neural Information Processing Systems*, 27, 2014.
- Jamie Hayes and George Danezis. Generating steganographic images via adversarial training. *Advances in Neural Information Processing Systems*, 30, 2017.
- Amir Hertz, Sharon Fogel, Rana Hanocka, Raja Giryes, and Daniel Cohen-Or. Blind visual motif removal from a single image. In *Proceedings of the IEEE/CVF Conference on Computer Vision and Pattern Recognition*, pages 6858–6867, 2019.
- Jonathan Ho, Ajay Jain, and Pieter Abbeel. Denoising diffusion probabilistic models, 2020. URL <https://arxiv.org/abs/2006.11239>.
- Osama Hosam. Attacking image watermarking and steganography—a survey. *International Journal of Information Technology and Computer Science*, 11(3):23–37, 2019.
- Zhengyuan Jiang, Jinghui Zhang, and Neil Zhenqiang Gong. Evading watermark based detection of ai-generated content. In *Proceedings of the 2023 ACM SIGSAC Conference on Computer and Communications Security*, pages 1168–1181, 2023.
- Zhengyuan Jiang, Moyang Guo, Yuepeng Hu, and Neil Zhenqiang Gong. Watermark-based detection and attribution of ai-generated content. *arXiv preprint arXiv:2404.04254*, 2024.
- Bahjat Kawar, Shiran Zada, Oran Lang, Omer Tov, Huiwen Chang, Tali Dekel, Inbar Mosseri, and Michal Irani. Imagic: Text-based real image editing with diffusion models. In *Proceedings of the IEEE/CVF Conference on Computer Vision and Pattern Recognition*, pages 6007–6017, 2023.
- Changhoon Kim, Kyle Min, Maitreya Patel, Sheng Cheng, and Yezhou Yang. Wouaf: Weight modulation for user attribution and fingerprinting in text-to-image diffusion models. In *Proceedings of the IEEE/CVF Conference on Computer Vision and Pattern Recognition*, pages 8974–8983, 2024.
- John Kirchenbauer, Jonas Geiping, Yuxin Wen, Jonathan Katz, Ian Miers, and Tom Goldstein. A watermark for large language models. In *International Conference on Machine Learning*, pages 17061–17084. PMLR, 2023.
- Alex Krizhevsky, Ilya Sutskever, and Geoffrey E Hinton. Imagenet classification with deep convolutional neural networks. *Advances in Neural Information Processing Systems*, 25, 2012.
- Xiang Li, Chan Lu, Danni Cheng, Wei-Hong Li, Mei Cao, Bo Liu, Jiechao Ma, and Wei-Shi Zheng. Towards photo-realistic visible watermark removal with conditional generative adversarial networks. In *Image and Graphics: 10th International Conference, ICIG 2019, Beijing, China*,

- August 23–25, 2019, *Proceedings, Part I 10*, pages 345–356. Springer, 2019.
- Jing Liang, Li Niu, Fengjun Guo, Teng Long, and Liqing Zhang. Visible watermark removal via self-calibrated localization and background refinement. In *Proceedings of the 29th ACM international conference on multimedia*, pages 4426–4434, 2021.
- Feng Lin and Robert D Brandt. Towards absolute invariants of images under translation, rotation, and dilation. *Pattern Recognition Letters*, 14(5):369–379, 1993.
- Yang Liu, Zhen Zhu, and Xiang Bai. Wdnet: Watermark-decomposition network for visible watermark removal. In *Proceedings of the IEEE/CVF winter conference on applications of computer vision*, pages 3685–3693, 2021.
- Aleksander Madry, Aleksandar Makelov, Ludwig Schmidt, Dimitris Tsipras, and Adrian Vladu. Towards deep learning models resistant to adversarial attacks. In *International Conference on Learning Representations*, 2018.
- Kartik Narayan, Harsh Agarwal, Kartik Thakral, Surbhi Mittal, Mayank Vatsa, and Richa Singh. Df-platter: Multi-face heterogeneous deepfake dataset. In *Proceedings of the IEEE/CVF Conference on Computer Vision and Pattern Recognition*, pages 9739–9748, 2023.
- JJK ó Ruanaidh, WJ Dowling, and FM Boland. Watermarking digital images for copyright protection. *IEEE Proceedings Vision Image and Signal Processing*, 143: 250–256, 1996.
- Mikhail Pautov, Nikita Bogdanov, Stanislav Pyatkin, Oleg Rogov, and Ivan Oseledets. Probabilistically robust watermarking of neural networks. In *Proceedings of the Thirty-Third International Joint Conference on Artificial Intelligence*, pages 4778–4787, 2024.
- Edgar Riba, Dmytro Mishkin, Daniel Ponsa, Ethan Rublee, and Gary Bradski. Kornia: an open source differentiable computer vision library for pytorch. In *Proceedings of the IEEE/CVF Winter Conference on Applications of Computer Vision*, pages 3674–3683, 2020.
- Robin Rombach, Andreas Blattmann, Dominik Lorenz, Patrick Esser, and Björn Ommer. High-resolution image synthesis with latent diffusion models. In *Proceedings of the IEEE/CVF Conference on Computer Vision and Pattern Recognition*, pages 10684–10695, 2022.
- Nataniel Ruiz, Yuanzhen Li, Varun Jampani, Yael Pritch, Michael Rubinstein, and Kfir Aberman. Dreambooth: Fine tuning text-to-image diffusion models for subject-driven generation. In *Proceedings of the IEEE/CVF Conference on Computer Vision and Pattern Recognition*, pages 22500–22510, 2023.
- Chitwan Saharia, William Chan, Saurabh Saxena, Lala Li, Jay Whang, Emily L Denton, Kamyar Ghasemipour, Raphael Gontijo Lopes, Burcu Karagol Ayan, Tim Salimans, et al. Photorealistic text-to-image diffusion models with deep language understanding. *Advances in Neural Information Processing Systems*, 35:36479–36494, 2022.
- Flavio Schneider, Ojasv Kamal, Zhijing Jin, and Bernhard Schölkopf. Moûsai: Efficient text-to-music diffusion models. In *Proceedings of the 62nd Annual Meeting of the Association for Computational Linguistics (Volume 1: Long Papers)*, pages 8050–8068, 2024.
- Richard Shin. Jpeg-resistant adversarial images. 2017. URL <https://api.semanticscholar.org/CorpusID:204804905>.
- Jascha Sohl-Dickstein, Eric A. Weiss, Niru Maheswaranathan, and Surya Ganguli. Deep unsupervised learning using nonequilibrium thermodynamics, 2015. URL <https://arxiv.org/abs/1503.03585>.
- Ruizhou Sun, Yukun Su, and Qingyao Wu. Denet: disentangled embedding network for visible watermark removal. In *Proceedings of the AAAI Conference on Artificial Intelligence*, volume 37, pages 2411–2419, 2023.
- Olga Taran, Shideh Rezaeifar, Taras Holotyak, and Slava Voloshynovskiy. Defending against adversarial attacks by randomized diversification. In *Proceedings of the IEEE/CVF Conference on Computer Vision and Pattern Recognition (CVPR)*, June 2019.
- Zijie J. Wang, Evan Montoya, David Munechika, Haoyang Yang, Benjamin Hoover, and Duen Horng Chau. DiffusionDB: A large-scale prompt gallery dataset for text-to-image generative models. *arXiv:2210.14896 [cs]*, 2022. URL <https://arxiv.org/abs/2210.14896>.
- Yuxin Wen, John Kirchenbauer, Jonas Geiping, and Tom Goldstein. Tree-rings watermarks: Invisible fingerprints for diffusion images. *Advances in Neural Information Processing Systems*, 36, 2024.
- Hanzhou Wu, Gen Liu, Yuwei Yao, and Xinpeng Zhang. Watermarking neural networks with watermarked images. *IEEE Transactions on Circuits and Systems for Video Technology*, 31(7):2591–2601, 2020.
- Chaoran Xu, Yao Lu, and Yuanpin Zhou. An automatic visible watermark removal technique using image inpainting algorithms. In *2017 4th International Conference on Systems and Informatics (ICSAI)*, pages 1152–1157. IEEE, 2017.
- Binxin Yang, Shuyang Gu, Bo Zhang, Ting Zhang, Xuejin Chen, Xiaoyan Sun, Dong Chen, and Fang Wen. Paint by example: Exemplar-based image editing with diffusion models. In *Proceedings of the IEEE/CVF Conference on*

Computer Vision and Pattern Recognition, pages 18381–18391, 2023.

Ning Yu, Vladislav Skripniuk, Sahar Abdelnabi, and Mario Fritz. Artificial fingerprinting for generative models: Rooting deepfake attribution in training data. In *Proceedings of the IEEE/CVF International Conference on Computer Vision*, pages 14448–14457, 2021.

Lijun Zhang, Xiao Liu, Antoni Viros Martin, Cindy Xiong Bearfield, Yuriy Brun, and Hui Guan. Robust image watermarking using stable diffusion. *arXiv preprint arXiv:2401.04247*, 2024.

Lvmin Zhang, Anyi Rao, and Maneesh Agrawala. Adding conditional control to text-to-image diffusion models. In *Proceedings of the IEEE/CVF International Conference on Computer Vision*, pages 3836–3847, 2023.

Richard Zhang, Phillip Isola, Alexei A Efros, Eli Shechtman, and Oliver Wang. The unreasonable effectiveness of deep features as a perceptual metric. In *CVPR*, 2018.

Hanqing Zhao, Wenbo Zhou, Dongdong Chen, Tianyi Wei, Weiming Zhang, and Nenghai Yu. Multi-attentional deepfake detection. In *Proceedings of the IEEE/CVF Conference on Computer Vision and Pattern Recognition*, pages 2185–2194, 2021.

Xuandong Zhao, Prabhanjan Vijendra Ananth, Lei Li, and Yu-Xiang Wang. Provable robust watermarking for ai-generated text. In *The Twelfth International Conference on Learning Representations*, 2024.

Yunqing Zhao, Tianyu Pang, Chao Du, Xiao Yang, Ngai-Man Cheung, and Min Lin. A recipe for watermarking diffusion models. *arXiv preprint arXiv:2303.10137*, 2023.

Jiren Zhu, Russell Kaplan, Justin Johnson, and Li Fei-Fei. Hidden: Hiding data with deep networks. In *Computer Vision - ECCV 2018 - 15th European Conference, Munich, Germany, September 8-14, 2018, Proceedings, Part XV*, volume 11219, pages 682–697, 2018.

Spread them Apart: Towards Robust Watermarking of Generated Content (Supplementary Material)

Mikhail Pautov^{1,2*}

Danil Ivanov^{3*}

Andrey V. Galichin^{1,3}

Oleg Rogov^{1,3,4}

Ivan Oseledets^{1,3}

¹AIRI, Moscow, Russia

²ISP RAS Research Center for Trusted AI, Moscow, Russia

³Skolkovo Institute of Science and Technology, Moscow, Russia

⁴Moscow Technical University of Communications and Informatics, Moscow, Russia

A IMPROVING THE ROBUSTNESS TO WATERMARK REMOVAL ATTACKS

Note that the version of the watermarking method proposed in this paper is based on the embedding of the watermark into the pixel domain of a generated image. Hence, the method can not yield watermarks provably robust against geometric transformations of the image, such as rotations and translations. In this section, we describe an extension of the method to guarantee robustness against such transformations. An extension is done by embedding the watermark simultaneously into the pixel domain and special representations in the frequency domain, which are invariant under rotations and translations.

A.1 INVARIANTS IN THE FREQUENCY DOMAIN

We will call image transform $\gamma : \mathbb{R}^d \rightarrow \mathbb{R}^d$ *invariant* under parametric perturbation $\phi : \mathbb{R}^d \times \Theta \rightarrow \mathbb{R}^d$ at point $x \in \mathbb{R}^d$ if

$$\gamma(x) = \gamma(\phi(x, \theta)) \quad \text{for all } \theta \in \Theta, \quad (18)$$

where Θ is the set of parameters of perturbation ϕ . In this work, we use two invariants discussed in Lin and Brandt [1993], formulated as theorems below.

Theorem A.1. *Let $h(x, y)$ be an integrable nonnegative function and its Fourier transform*

$$H(\omega_x, \omega_y) = \int_{-\infty}^{\infty} \int_{-\infty}^{\infty} h(x, y) e^{-i(x\omega_x + y\omega_y)} dx dy = A(\omega_x, \omega_y) e^{-i\psi(\omega_x, \omega_y)} \quad (19)$$

be twice differentiable. Then the function $A(\omega_x, \omega_y)$ is invariant under translation.

Theorem A.2. *Let $\tilde{h}(r, t) = h(e^r \cos t, e^r \sin t)$ be the logarithmic-polar representation of the image $h(x, y)$. The Fourier-Mellin transform of $\tilde{h}(r, t)$ is*

$$\tilde{H}(\omega, k) = \int_{-\infty}^{\infty} \int_0^{2\pi} \tilde{h}(r, t) e^{-i(kt + \omega r)} dt dr = \tilde{A}(\omega, k) e^{-i\tilde{\psi}(\omega, k)}, \quad (20)$$

where $\tilde{A}(\omega, k)$ is the magnitude and $\tilde{\psi}(\omega, k)$ is the phase.

If $\tilde{h}(r, t)$ is an integrable nonnegative function and its Fourier-Mellin transform $\tilde{H}(\omega, k)$ is twice differentiable, then the function $\tilde{A}(\omega, k)$ is invariant under rotation.

Remark. *For consistent notation, we assume that the image $h(x, y)$ is a scalar function on a two-dimensional plane. Later, we refer to invariants from Theorems A.1-A.2 as to γ_t and γ_r , respectively.*

A.2 SPREAD THEM APART: THREE WATERMARKS INSTEAD OF ONE

Recall from Section 4 that the watermark embedding process in the pixel domain is done by optimizing the loss function \mathcal{L} in the form from Eq. 10: $\mathcal{L} = \lambda_{wm}\mathcal{L}_{wm} + \lambda_{qual}\mathcal{L}_{qual}$, where

$$\mathcal{L}_{wm} = \sum_{i=1}^n \min((-1)^{w_i}(x_{a_i} - x_{b_i}) + \varepsilon, 0), \quad x = \mathcal{D}(z), \quad (21)$$

$w(u_i) = \{w_1, \dots, w_n\}$ is the watermark assigned to user u_i and $s(u_i) = \{a_1, \dots, a_n, b_1, \dots, b_n\}$ is the secret of user u_i .

To ensure the robustness of the watermark to geometric transformations, we suggest embedding the watermark simultaneously in the pixel domain and in invariants γ_t and γ_r . To do so, we optimize the loss function $\tilde{\mathcal{L}}$ in the form below:

$$\tilde{\mathcal{L}} = \lambda_{wm}\mathcal{L}_{wm} + \lambda_{qual}\mathcal{L}_{qual} + \lambda_t\mathcal{L}_t + \lambda_r\mathcal{L}_r = \mathcal{L} + \lambda_t\mathcal{L}_t + \lambda_r\mathcal{L}_r. \quad (22)$$

In Eq. 22, λ_t , λ_r are positive constants and

$$\mathcal{L}_t = \sum_{i=1}^n \min((-1)^{w_i}(\gamma_t(x)_{a_i} - \gamma_t(x)_{b_i}) + \varepsilon, 0), \quad (23)$$

$$\mathcal{L}_r = \sum_{i=1}^n \min((-1)^{w_i}(\gamma_r(x)_{a_i} - \gamma_r(x)_{b_i}) + \varepsilon, 0) \quad (24)$$

are the loss functions that control the embedding of the watermark into invariants $\gamma_t(x)$ and $\gamma_r(x)$, respectively.

A.3 EXTRACTIONS OF WATERMARKS

Given m as the number of users, the owner of the generative model extracts $3m$ watermarks from the given image x . Namely, given the secret $s(u_i)$ of the user u_i , three watermarks, $w(u_i|x)$, $w(u_i|\gamma_r(x))$, $w(u_i|\gamma_t(x))$ are restored:

$$\begin{cases} x_{a_j} \geq x_{b_j} \implies w(u_i|x)_j = 0, \\ x_{a_j} < x_{b_j} \implies w(u_i|x)_j = 1, \end{cases} \quad (25)$$

$$\begin{cases} \gamma_r(x)_{a_j} \geq \gamma_r(x)_{b_j} \implies w(u_i|\gamma_r(x))_j = 0, \\ \gamma_r(x)_{a_j} < \gamma_r(x)_{b_j} \implies w(u_i|\gamma_r(x))_j = 1, \end{cases} \quad (26)$$

$$\begin{cases} \gamma_t(x)_{a_j} \geq \gamma_t(x)_{b_j} \implies w(u_i|\gamma_t(x))_j = 0, \\ \gamma_t(x)_{a_j} < \gamma_t(x)_{b_j} \implies w(u_i|\gamma_t(x))_j = 1. \end{cases} \quad (27)$$

To assign the (possibly) watermarked image x to the user, the owner of the model determines three candidates:

$$\begin{cases} u = \arg \min_{u_i \in \{u_1, \dots, u_m\}: \xi_i = 1} d(w(u_i), w(u_i|x)), \\ u_r = \arg \min_{u_i \in \{u_1, \dots, u_m\}: \xi_i^r = 1} d(w(u_i), w(u_i|\gamma_r(x))), \\ u_t = \arg \min_{u_i \in \{u_1, \dots, u_m\}: \xi_i^t = 1} d(w(u_i), w(u_i|\gamma_t(x))), \end{cases} \quad (28)$$

where

$$\xi_i^p = \mathbb{1}[d(w(u_i|\gamma_p(x)), w(u_i)) \in [0, \tau_1] \cup [\tau_2, n]] \quad (29)$$

indicates which of the users' watermarks are within an appropriate distance from the corresponding extracted watermarks.

Finally, the owner of the model assigns the image x to the user \tilde{u} that corresponds to the minimum distance among all $3m$ pairs of watermarks:

$$\tilde{u} = \arg \min \{d(w(u), w(u|x)), d(w(u_r), w(u_r|\gamma_r(x))), d(w(u_t), w(u_t|\gamma_t(x)))\}. \quad (30)$$

A.4 PROBABILITY OF INCORRECT ATTRIBUTION

Assume that the user u_i owns the watermarked image x . Note that the attribution of the image to the user u_i is guaranteed to hold if

$$u = u_i, u_r = u_i, u_t = u_i. \quad (31)$$

Hence, the probability of incorrect attribution, $FPR_3(m)$, is bounded from above by the sum

$$\mathbb{P}(u \neq u_i) + \mathbb{P}(u_r \neq u_i) + \mathbb{P}(u_t \neq u_i), \quad (32)$$

yielding

$$FRP_3(m) \leq 3\hat{p}, \quad (33)$$

where \hat{p} is from Eq. 4.

A.5 QUANTITATIVE RESULTS

In Tables 5-6, we include rotation and translation transformations of the image. To rotate an image, we sample an angle of rotation θ_r uniformly from $[-10^\circ, 10^\circ]$; to translate an image, we sample the vector of translation (θ_t^x, θ_t^y) uniformly from the set $[-10^\circ, 10^\circ] \times [-10^\circ, 10^\circ]$. We compare the results of an extended version of the proposed method with the baseline approach. STA(1) refers to the baseline approach described in Section 4, STA(3) refers to an extended approach described in Section A. Note that now, according to Section A.4, to achieve $FPR = 10^{-6}$ we set $\tau_1 = 24$ and $\tau_2 = 76$. In the column ‘‘Error’’, we report the bit-wise accuracy of the watermarking procedure.

To focus on the evaluation of the robustness of the watermarks, we report results for the images in which the watermark is embedded successfully. Namely, after embedding the watermark, we choose the watermarked images with a generation error smaller than 0.05.

It is noteworthy that the simultaneous embedding of the watermark into the pixel domain and corresponding invariants in the frequency domain significantly improves the robustness against post-processing watermark removal attacks. The limitation of this approach is the increased complexity of the watermark embedding process which is the subject of future work.

Table 5: TPRs under different types of watermark removal attacks, attribution problem. We use $k = 10$ different private keys and fix $FPR = 10^{-6}$. The best results are highlighted in **bold**.

Method	Error	Brightness	Contrast +	Contrast -	Gamma	JPEG	Translation
STA(1)	0.972	0.928	0.928	0.928	0.928	0.724	0.000
STA(3)	0.980	1.000	1.000	1.000	0.951	0.563	0.962
Method	Hue	Saturation	Sharpness	Noise	PGD	Rotation	
STA(1)	1.000	0.571	1.000	0.928	0.857	0.000	
STA(3)	1.000	1.000	1.000	0.928	0.857	0.489	

Table 6: TPRs under different types of watermark removal attacks, detection problem. We use $k = 10$ different private keys and fix $FPR = 10^{-6}$. The best results are highlighted in **bold**.

Method	Error	Brightness	Contrast +	Contrast -	Gamma	JPEG	Translation
STA(1)	0.972	0.928	0.928	0.928	0.928	0.724	0.000
STA(3)	0.980	1.000	1.000	1.000	0.951	0.563	0.962
Method	Hue	Saturation	Sharpness	Noise	PGD	Rotation	
STA(1)	1.000	0.571	1.000	0.928	0.857	0.000	
STA(3)	1.000	1.000	1.000	0.928	0.857	0.489	